

EXCEPTIONAL SURGERIES ON ALTERNATING KNOTS

KAZUHIRO ICHIHARA AND HIDETOSHI MASAI

Dedicated to Professor Sadayoshi Kojima on the occasion of his 60th birthday

ABSTRACT. We give a complete classification of exceptional surgeries on hyperbolic alternating knots in the 3-sphere. As an appendix, we also show that the Montesinos knots $M(-1/2, 2/5, 1/(2q+1))$ with $q \geq 5$ have no non-trivial exceptional surgeries. This gives the final step in a complete classification of exceptional surgeries on arborescent knots.

CONTENTS

1. Introduction	1
2. Preliminaries	4
3. Proof of Corollary 1.2	5
4. Proof of Theorem 1.1	6
5. Reducing the number of augmented links and components	9
6. Procedures for Computer-aided calculations	18
Acknowledgements	24
Appendix A. Verified Computation	24
Appendix B. A family of Montesinos knots	25
References	29

1. INTRODUCTION

The well-known Hyperbolic Dehn Surgery Theorem due to Thurston [45, Theorem 5.8.2.] says that each hyperbolic knot (i.e., a knot with the complement admitting a hyperbolic structure) admits only finitely many Dehn surgeries yielding non-hyperbolic manifolds. In view of this, such finitely many exceptions are called *exceptional surgeries*.

A complete classification of exceptional surgeries on hyperbolic knots in the 3-sphere remains an important and difficult challenge in both Knot Theory and 3-manifold topology. However, such a classification is known for some infinite families of knots. For example, a classification of exceptional surgeries on hyperbolic 2-bridge knots was obtained in [7]. Quite recently, exceptional surgeries on hyperbolic pretzel knots were also classified in [29].

In this paper, we consider exceptional surgeries on hyperbolic alternating knots in S^3 , one of the most well-known classes of knots. A knot in S^3 is called *alternating* if

Ichihara is partially supported by JSPS KAKENHI Grant Number 23740061.

The work of Masai is partially supported by JSPS Research Fellowship for Young Scientists.

it admits a diagram with alternatively arranged over-crossings and under-crossings running along it.

The main theorem of this paper is:

Theorem 1.1. *Let K be a hyperbolic alternating knot in the 3-sphere. If K admits a non-trivial exceptional surgery, then K is equivalent to an arborescent knot.*

The definition of arborescent knots together with other definitions and background is delayed until §2.

Recently, exceptional surgeries on (both alternating and non-alternating) arborescent knots have been almost classified. Building on these partial results, we provide a complete classification of exceptional surgeries on alternating knots as a corollary of our theorem.

Corollary 1.2. *Let K be a hyperbolic alternating knot in S^3 . Suppose that the manifold $K(r)$ obtained by Dehn surgery on K along a non-trivial slope r is non-hyperbolic for some rational number r . Then r must be an integer and $K(r)$ is irreducible. Furthermore the following hold. If $K(r)$ is toroidal, then $K(r)$ is not a Seifert fibered, and K is equivalent to either*

- the figure-eight knot and $r = 0, \pm 4$,
- a two bridge knot $K_{[b_1, b_2]}$ with $|b_1|, |b_2| > 2$, and $r = 0$ if both b_1, b_2 are even, $r = 2b_2$ if b_1 is odd and b_2 is even,
- a twist knot $K_{[2n, \pm 2]}$ with $|n| > 1$ and $r = 0, \mp 4$,
- a pretzel knot $P(q_1, q_2, q_3)$ with $q_i \neq 0, \pm 1$ for $i = 1, 2, 3$, and $r = 0$ if q_1, q_2, q_3 are all odd, $r = 2(q_2 + q_3)$ if q_1 is even and q_2, q_3 are odd.

In the above, when $r \neq 0$, then r is always a boundary slope of a once punctured Klein bottle spanned by K . If $K(r)$ is small Seifert fibered, then $K(r)$ has the infinite fundamental group, and K is equivalent to either

- the figure-eight knot and $r = \pm 1, \pm 2, \pm 3$,
- a twist knot $K_{[2n, \pm 2]}$ with $|n| > 1$ and $r = \mp 1, \mp 2, \mp 3$.

In particular, the figure-eight knot is the only knot admitting 10 exceptional surgeries among hyperbolic alternating knots, and the others admit at most 5 exceptional surgeries.

The proof of this corollary is given in Section 3. The last assertion immediately follows from the classification above, which gives an affirmative solution for alternating knots to the famous Gordon's conjecture: A hyperbolic manifold admits 10 exceptional fillings if and only if it is the figure 8 knot complement, and otherwise, it admits fewer exceptional fillings. It was shown in [16] based on [15] that any hyperbolic alternating knot in S^3 has at most 10 exceptional surgeries, and recently, Lackenby and Meyerhoff [24] proved in general that any hyperbolic knot in any closed 3-manifold has at most 10 exceptional surgeries. On the other hand, as stated in [22, Problem 1.77], Gordon conjectured that only the figure-eight knot attains the maximal, that is 10, but the methods used in the above papers could not prove this.

We remark that our proof of Theorem 1.1 is computer-aided. In Section 4, we will give an outline of our proof, and, in particular, we will clarify where we used computer in the proof. Actually, due to [23], we have only finitely many (but a

huge number of) links so that Theorem 1.1 follows from the complete classification of certain types of exceptional surgeries on them. Thus our task is to investigate the surgeries on these finite number of links.

In Section 5, we will discuss how to reduce the number of the links which we have to check. As is explained in Section 6, by computer-aided calculations, we have a potential procedure to rigorously verify that a given link admits no non-trivial exceptional surgeries. However applying it for all the links obtained by using [23] alone is computationally expensive. Therefore we give a number of observations to reduce the number of links we need to check, which we estimated to be in the millions. First, we consider symmetries of the links and the other diagrammatic arguments in order to reduce this number. To further reduce the number of links and the number of components for some of the links, we applied some techniques and results of [51], which use essential laminations in the link exteriors. Even with these reductions, the size of the computation is outside the scope of a personal computer. As noted above, the verification needed for each link is an involved process. To be more specific, we have about 30,000 links to investigate, and for each link, we have to apply the procedure developed in [13] recursively. In fact, in the worst case, we have to apply the procedure more than 18,000 times. Therefore, we ran our computations on the super-computer, “TSUBAME”, housed at Tokyo Institute of Technology. The result of all the computations verifies that none of the links admit unexpected non-trivial exceptional surgeries.

In Section 6, we will explain our main code `fef.py` (short for `find exceptional fillings`) that rigorously ensures the non-existence of non-trivial exceptional surgeries of certain type. The code and the outputs of the program are downloadable from [20]. We will explain the procedure of our code in detail, including information about computation environments used during our computation. Our program is essentially based on the technique developed in [26]¹. The code for the first version of [26] did not account for round-off error properly. To obtain mathematically rigorous computations, we improved their code using verified numerical analysis based on interval arithmetic. Some fundamentals about such methods will be given in Appendix A. The key step to show that the links have no exceptional surgeries is to prove the hyperbolicity of a given manifold rigorously. A technique to prove the hyperbolicity via computer has been developed in [13] by the team containing the authors of this paper.

Actually our computer assisted part of the proof of Theorem 1.1 can be adapted to provide the final step needed to classify all exceptional surgeries on hyperbolic arborescent knots. In Appendix B, applying our method of obtaining a complete classification of exceptional surgeries on a given hyperbolic link, we show that the Montesinos knots $M(-1/2, 2/5, 1/(2q + 1))$ with $q \geq 5$ have no non-trivial exceptional surgeries. This gives the final step in a complete classification of exceptional surgeries on arborescent knots. We remark that these computations can be done without using the super-computer “TSUBAME”.

Remark 1. We here remark that prime alternating knots are known to be all hyperbolic except for $(2, p)$ -torus knots, that is, knots isotoped to the $(2, p)$ -curves on the standardly embedded torus in S^3 . Actually Menasco showed in [30, Corollary 2] a non-split prime alternating link which is not a torus link has the complement admitting a complete hyperbolic structure of finite volume, and Murasugi showed

¹Recently, they updated their paper and code to use our technique. See Version 2 of [26].

in [34, Theorem 3.2] that the torus knots of type $(2, p)$ are only alternating knots among all torus knots by calculating Alexander polynomials. Also note that a purely geometric proof of the latter was obtained by Menasco and Thistlethwaite [31, Corollary 2].

Remark 2. For the proof of Theorem 1.1, we used the code named “fef.py” which is specially customized for alternating knots. The code named “fef_gen.py” which we used in Appendix B works for any cusped hyperbolic 3-manifolds. Both code are included the package available at [20].

2. PRELIMINARIES

2.1. Dehn surgery. By a *Dehn surgery* on a knot K , we mean the following operation to create a new 3-manifold from a given one and a given knot: first remove an open tubular neighborhood of K to obtain the *exterior* $E(K)$ of K , and glue a solid torus V back via a boundary homeomorphism $f : \partial V \rightarrow \partial E(K)$. We say the isotopy class of each non-trivial unoriented simple closed curve in $\partial E(K)$ is a *slope*. We pay special attention to the slope γ that is identified to the isotopy class of curves in ∂V that bounds a disk in V . In this context, we call γ the *surgery slope* (see [40] for further details and background on Dehn surgery). When K is a knot in S^3 , by using the standard meridian-longitude system, slopes on $\partial E(K)$ are parametrized by $\mathbb{Q} \cup \{1/0\}$. For example, the meridian of K corresponds to $1/0$ and the longitude to 0 . We thus denote by $K(r)$ the 3-manifold obtained by Dehn surgery on a knot K along a slope corresponding to a rational number r . By the *trivial* Dehn surgery on K in S^3 , we mean the Dehn surgery on K along the meridional slope $1/0$. Thus, it yields S^3 again, which is obviously exceptional, when K is hyperbolic. We say that a Dehn surgery on K in S^3 is *integral* if it is along an integral slope. This means that the curve representing the surgery slope runs longitudinally once.

We also recall a classification of exceptional surgeries. As a consequence of the famous Geometrization Conjecture, raised by Thurston in [46, section 6, question 1], and established by Perelman’s works, [37], [38], [39], all closed orientable 3-manifolds are classified as: reducible (i.e., containing 2-spheres not bounding 3-balls), toroidal (i.e., containing incompressible tori), Seifert fibered (i.e., foliated by circles), or hyperbolic (i.e., admitting a complete Riemannian metric with constant sectional curvature -1). See [42] for a survey. Thus, exceptional surgeries are also divided into three types; reducible (i.e., yielding a reducible manifold), toroidal (i.e., yielding a toroidal manifold), or Seifert fibered (i.e., yielding a Seifert fibered manifold).

2.2. Families of knots. We here introduce some notions for knots that we use in this paper.

A *bridge index* of a knot in S^3 is defined as the minimal number of local maxima (or local minima) up to ambient isotopy. Thus, a knot with bridge index 2 is called a *two-bridge knot*. Since two-bridge knots are alternating, a natural consequence of Menasco’s work in [30] is that a two-bridge knot is hyperbolic unless it is a $(2, p)$ -torus knot.

We now recall some standard notation and terminology regarding arborescent knots. See [48] for full details. By a *tangle*, we mean a pair with a 3-ball and properly embedded 1-manifolds. From two arcs of rational slope drawn on the

boundary of a pillowcase-shaped 3-ball, one can obtain a tangle, which is called a *rational tangle*. A tangle obtained by putting rational tangles together in a horizontal way is called a *Montesinos tangle*. An *arborescent tangle* is then defined as a tangle that can be obtained by summing several Montesinos tangles together in an arbitrary order.

Suppose that a knot K in S^3 is obtained by closing a tangle T . If T is a Montesinos tangle, then we call K a *Montesinos knot*, and if T is an arborescent tangle, then we call K an *arborescent knot*.

The number of rational tangles forming the corresponding Montesinos tangle is called the *length* of the Montesinos knot. It is seen that prime Montesinos knots with length at most two are all two-bridge knots. Thus, they are all alternating. On the other hand, Montesinos knots of length at least three are generally not alternating.

In [48], Wu divided all arborescent knots into three types: *type I* knots - two-bridge knots or Montesinos knots of length 3, *type II* knots - the union of two Montesinos tangles, each of which is formed by two rational tangles corresponding to $1/2$ and a non-integer, and all the other arborescent knots are *type III*.

We denote by $M(r_1, r_2, \dots, r_n)$ a Montesinos knot constructed from rational tangles corresponding to rational numbers r_1, r_2, \dots, r_n . In particular, $M(1/q_1, 1/q_2, \dots, 1/q_n)$ with integers q_1, q_2, \dots, q_n is called a *pretzel knot* of n -strands.

3. PROOF OF COROLLARY 1.2

Let K be a hyperbolic alternating knot in S^3 . Suppose that the surgered manifold $K(r)$ is non-hyperbolic for some rational number r . As we recall above, we see that $K(r)$ is reducible, toroidal or Seifert fibered.

First, r must be an integer by the first author in [16, Theorem 1.1].

Also, $K(r)$ must be irreducible by Menasco and Thistlethwaite [31, Corollary 1.1].

Suppose that $K(r)$ is toroidal. Then $K(r)$ is not Seifert fibered, shown by the first author with Jong [18]. Moreover, as a consequence of the argument used in the classification of toroidal surgeries on alternating knots obtained by Patton [36] and Boyer and Zhang [3, Lemma 3.1], we see that K and r is a pair listed in the statement of Corollary 1.2. Alternatively, this observation also follows from our Theorem 1.1, together with the classifications of toroidal surgeries on two-bridge knots and other arborescent knots obtained by Brittenham and Wu [7] and Wu [49], [50].

Suppose that $K(r)$ is Seifert fibered. As noted above, by [18], $K(r)$ must be small Seifert fibered. Also, as shown in [9], $K(r)$ has infinite fundamental group. Moreover, by Theorem 1.1, K is an arborescent knot. Any hyperbolic arborescent knot of type II or type III cannot admit a small Seifert fibered surgery by Wu in [48], [50]. Thus, K must be an arborescent knot of type I, and so K is either a two-bridge knot or a Montesinos knot of length 3.

If K is a two-bridge knot, then K is either the figure-eight knot and $r = \pm 1, \pm 2, \pm 3$ or a twist knot $K_{[2n, \pm 2]}$ with $|n| > 1$ and $r = \mp 1, \mp 2, \mp 3$ as claimed in the corollary by the result of Brittenham and Wu [7].

For Montesinos knots of length 3, except the particular family of Montesinos knots $M(-1/2, 2/5, 1/(2q+1))$ with $q \geq 5$, Meier obtained a complete classification of exceptional surgeries in [29]. Due to the classification, we see that all the

Montesinos knots of length three admitting small Seifert fibered surgeries are non-alternating as follows. Each of the knots can be checked that it admits reduced Montesinos diagrams which is non-alternating. Then the diagram is a minimal diagram, since if a Montesinos link admits an n -crossing reduced Montesinos diagram, then it cannot be projected with fewer than n crossings, as shown in [25, Theorem 10]. However, a non-alternating projection of a prime alternating link cannot be minimal [35, Theorem B], and so, the knots considered above are non-alternating. Finally we see that the Montesinos knots $M(-1/2, 2/5, 1/(2q+1))$ with $q \geq 5$ are non-alternating in the same way. This completes the proof of Corollary 1.2. \square

In Appendix B, we show that the Montesinos knots $M(-1/2, 2/5, 1/(2q+1))$ with $q \geq 5$ actually have no non-trivial exceptional surgeries.

4. PROOF OF THEOREM 1.1

Let K be a hyperbolic alternating knot in the 3-sphere. Suppose that K admits an exceptional surgery, i.e., suppose that the surgered manifold $K(r)$ is non-hyperbolic for some integer r .

First the following lemma, essentially due to Lackenby in [23, Theorem 5.1], shows that K is not “sufficiently complicated”.

Lemma 4.1. *If a hyperbolic alternating knot K has a connected prime alternating diagram D satisfying $t(D) \geq 9$, then K admits no non-trivial exceptional surgeries.*

In fact, Lackenby showed in [23, Theorem 5.1] that the knots satisfying the assumption above have no “non-hyperbolike” surgeries. Then the Perelman’s affirmative solution to the Geometrization Conjecture guarantees that “non-hyperbolike” is equivalent to non-hyperbolic, i.e., exceptional in this context.

Here we recall terminology used in the lemma above. Let D be a connected alternating diagram of a knot in S^3 , which we view as a 4-valent graph embedded in S^2 , equipped with “under-over” crossing information. Then D is called *prime* if each simple closed curve in S^2 intersecting D transversely in two points divides S^2 into two discs, one of which contains no crossings of D . The *twist number* of the diagram D , denoted by $t(D)$, is defined as the number of *twists*, which are either maximal connected collections of bigon regions in D arranged in a row or isolated crossings adjacent to no bigon regions.

In the case where $t(D) \leq 8$, we first have the following:

Lemma 4.2. *If a hyperbolic alternating knot K in S^3 has a connected prime alternating diagram D satisfying $t(D) \leq 8$, then either K is an arborescent knot or K has a connected prime alternating diagram D satisfying $6 \leq t(D) \leq 8$, and is obtained from one of the 9 plane graphs illustrated in Figure 1 by substituting one of the 4 tangles illustrated in Figure 2 to each of the fat vertices in the graphs, and performing twisting on all the augmented circles.*

Here we mean by an *augmented circle* an unknotted component which encircles a crossing or a pair of parallel two strands in a given diagram. Also we say that a knot is obtained by *twisting on an augmented circle* of a link if it is obtained by performing $1/q$ -surgery on the component ($q \in \mathbb{Z} \setminus \{0\}$).

Note that among the graphs in Figure 1, the top 3 graphs that will be named G_6, G_7, G_8^s are simple and 3-connected. Here a graph is said to be *simple* if it does

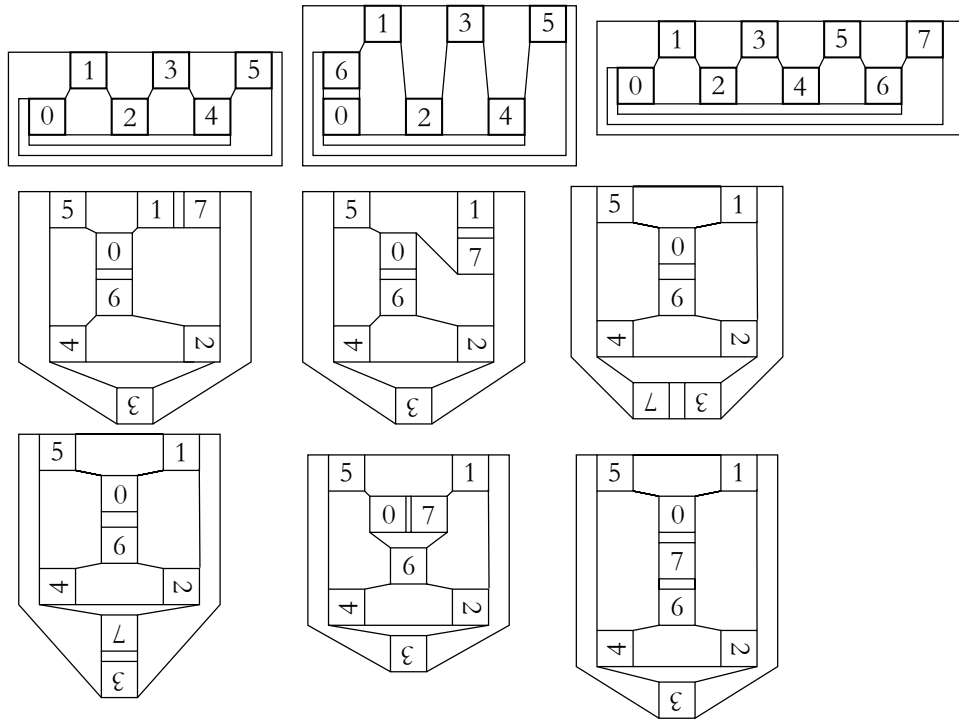


FIGURE 1. 9 plane graphs.

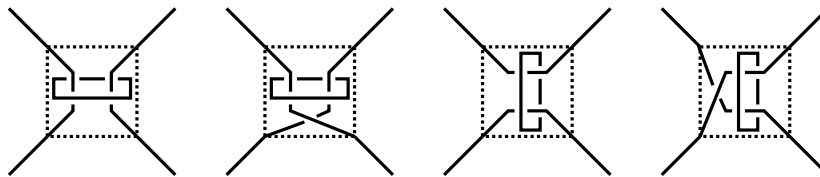


FIGURE 2. 4 tangles.

not have any multi edge or self loop, and *3-connected* if there does not exist a set of 2 vertices whose removal is disconnected.

Proof of Lemma 4.2. Let K be a hyperbolic alternating knot in S^3 , and D a connected prime alternating diagram of K . Suppose that K is not an arborescent knot and $t(D) \leq 8$.

As demonstrated in [23, Section 5], D is obtained from some regular 4-valent plane graph with $t(D)$ vertices by replacing all of its vertices with twists. It is equivalent to say that D is obtained from some regular 4-valent plane graph by substituting one of the 4 tangles illustrated in Figure 2 to each of the fat vertices in the graphs, and performing twisting on all the augmented circles. Now it suffices to show that, to obtain D , we only consider the 9 plane graphs depicted in Figure 1.

First we show that $t(D) \geq 6$. Suppose for a contrary that $t(D) \leq 5$. Then D is obtained from some regular 4-valent plane graph with at most 5 vertices. It is

well-known that such a plane graph always has a complementary bigon. See [4] for example. By collapsing a bigon to a ‘fat’ vertex, we have a new regular 4-valent plane graph with fewer vertices. Then the original diagram D is obtained by replacing all of its vertices with rational tangles or Montesinos tangles. Repeating this procedure, we have a regular 4-valent plane graph with a single vertex, from which we reconstruct the original diagram by replacing the vertex with an arborescent tangle. This means that the original D must represent an arborescent knot, contradicting the assumption that K is not an arborescent knot.

Next suppose that $t(D) = 6$. If D has a complementary bigon on the projection plane, then, in the same way as above, it is shown that D must represent an arborescent knot, contradicting the assumption. Thus D can admit no complementary bigons. Again, for example by [4], it is known that there is exactly one regular 4-valent plane graph, say G_6 , with 6 vertices without complementary bigons, which is depicted at the left of the top row in Figure 1.

Next suppose that $t(D) = 7$. Again, for example by [4], it is known that there is no regular 4-valent plane graph with 7 vertices without complementary bigons. This means that, under the assumption that D does not represent an arborescent knot, D is obtained from G_6 by replacing a vertex with a vertical or a horizontal bigon. Since G_6 is homogeneous, i.e. the graph automorphism group acts transitively on the set of vertices, it suffices to consider only one graph, say G_7 , which is depicted at the middle of the top row in Figure 1.

Finally suppose that $t(D) = 8$. Again, for example by [4], it is known that there is exactly one regular 4-valent plane graph with 8 vertices without complementary bigons, say G_8^s , which is depicted at the right of the top row in Figure 1. The other possibility is that D is obtained from G_6 by twice repetition of replacing a vertex with a vertical or a horizontal bigon. As mentioned above, G_7 is unique up to symmetry. Hence for this case we only need to add bigon to G_7 . By the symmetry of G_7 depicted in Figure 3, we see that there are 6 distinct ways to add bigons.

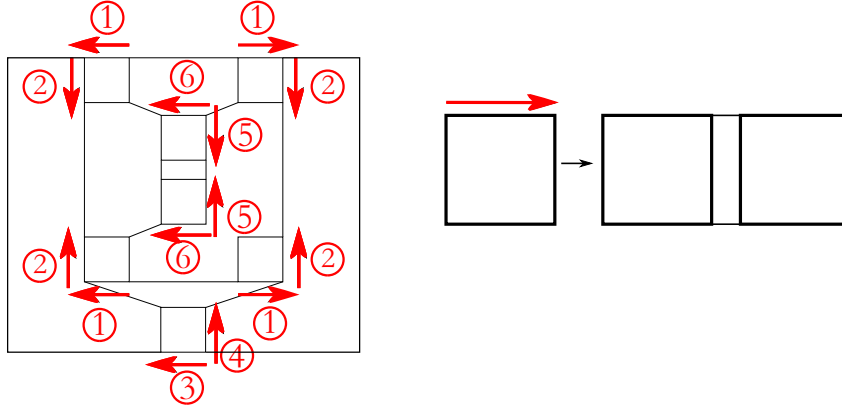


FIGURE 3. (left) 6 places and directions (up to symmetry) to add a bigon, (right) the meaning of arrows.

Those 6 graphs obtained by adding bigons to G_7 , say G_8^1, \dots, G_8^6 , are depicted at the middle and the bottom rows in Figure 1.

This completes the proof of the lemma. \square

The number of the links obtained above is naively estimated as $4^6 + 4^7 + 7 \cdot 4^8 = 479232$. The next lemma efficiently reduces the number of links we have to consider.

Lemma 4.3. *Let K be a hyperbolic alternating non-arborescent knot admitting a diagram D such that $6 \leq t(D) \leq 8$. Suppose that K admits a non-trivial exceptional surgery. Then there are 30404 hyperbolic links with augmented circles, which are constructed by substituting one of the 4 tangles in Figure 2 to each of the fat vertices of one of the 9 plane graphs in Figure 1, such that K is obtained from one of the links by performing twisting on the augmented circles.*

A proof of this lemma is given in the next section, which is computer-aided. The detailed explanation of the key piece of our code `twistLink.py`'s used in the proof is included. We actually have 9 files; `twistLink6.py`, `twistLink7.py`, `twistLink8.1.py`, `...`, `twistLink8.7.py`, one corresponds to a graph in Figure 1, and as a set we call them `twistLink.py`'s.

Lemma 4.4. *Let K be a knot obtained from a Dehn surgery on L , one of the 30404 augment links in S^3 obtained in Lemma 4.3, such that the surgery corresponds to twisting along the unknotted components of L . If K is alternating, then K is hyperbolic and admits no non-trivial exceptional surgeries.*

This lemma is proved by super-computer calculations, mainly by applying the program named `fef.py`. §6 is devoted to give detailed explanations of the code `fef.py`.

Now we are in the position to prove our main result.

Proof of Theorem 1.1. Let K be a hyperbolic alternating knot in S^3 . Suppose that K admits a non-trivial exceptional surgery. We show that K is equivalent to an arborescent knot.

Since K is hyperbolic, K is prime by [46, Corollary 2.2]. Let D be an alternating diagram of the knot K . Then D is connected since K is a knot (not a link). Since K is prime, the diagram D is also prime by [30, Theorem (b)].

Now we consider the twist number of the diagram D . By Lemma 4.1, if $t(D) \geq 9$, then K admits no non-trivial exceptional surgeries. Then, by combining Lemmas 4.2, 4.3, 4.4, any hyperbolic alternating non-arborescent knot in S^3 admits no non-trivial exceptional surgeries. \square

5. REDUCING THE NUMBER OF AUGMENTED LINKS AND COMPONENTS

In this section, we give a proof of Lemma 4.3. Throughout the section, assume K is a hyperbolic alternating non-arborescent knot K with a diagram D of twist number $t(D)$ satisfying $6 \leq t(D) \leq 8$ admitting a non-trivial exceptional surgery. Then we will show that there are 30404 hyperbolic links with augmented circles such that K is obtained from one of the links by performing twisting on the augmented circles.

The outline of this section is as follows. By Lemma 4.2, each of the links to be considered is obtained from one of the 9 plane graphs illustrated in Figures 1 by substituting one of the 4 tangles illustrated in Figure 2 to each of the fat vertices in the graphs, and performing twisting on all the augmented circles. In §5.1, we describe a method to encode and enumerate these links as sequences of elements in $\{0, 1, 2, 3\}$. In §5.2, we explain and enforce conditions on the sequences in order to reduce the number of links we need to investigate. To further reduce computation

time needed to prove Lemma 4.4, we will give a condition to reduce the number of components of the links so obtained. Our key ingredient is Lemma 5.1 based on the study of genuine laminations which remain genuine after any non-trivial Dehn surgery. This method extends the result of Wu in [51].

Together with considerations of our restrictions, we implemented our procedure as a set of files `twistLink.py`'s. All files used and data of outputs are available at [20]. In §5.4, we will explain these files. Note that our complete program has two parts. This part, used to prove Lemma 4.3, generates triangulation files of SnapPea. These files are then analyzed in the proof of Lemma 4.4, which will be explained in the next section.

5.1. Settings. We want to obtain the links with augmented circles such that any hyperbolic alternating non-arborescent knot with diagram D of twist number $t(D)$ satisfying $6 \leq t(D) \leq 8$ which admits a non-trivial exceptional surgery is obtained from one of the links by performing twisting on the augmented circles. By Lemma 4.2, such links are obtained from one of the 9 graphs $G_6, G_7, G_8^s, G_8^1, \dots, G_8^6$ in Figure 1. Note that each square with a figure in it is a vertex. We will call the square with i in it the i -th square.

We first explain how we relate such a link to a sequence of $\{0, 1, 2, 3\}$ of length l , where $l = 6, 7$, or 8 depending on the graph.

Let $\{a_i\}_{i=0}^{l-1}$ be one of such sequences. Then we fill the i -th square with a tangle according to the correspondence which is depicted in Figure 4. Namely, we fill i -th square with one of the two string tangle with an augmented circle such that the two strands connect

- (nw,sw) and (ne,se) respectively if $a_i = 0$,
- (nw,ne) and (sw,se) respectively if $a_i = 2$, or
- (nw,se) and (ne,sw) respectively if $a_i = 1$, or 3 ,

and the augmented circle is

- horizontal if $a_i \in \{0, 1\}$, or
- vertical if $a_i \in \{2, 3\}$.

Here nw corresponds to the north west corner of the square and we define ne, sw, and se similarly. Note that the orientation that determines nw, ne, sw, and se is determined by the orientation of the figure in it. We remark that there is an ambiguity of the sign of crossings when $a_i \equiv 1 \pmod{2}$. It will be explained in Remark 3 how to choose either of them.

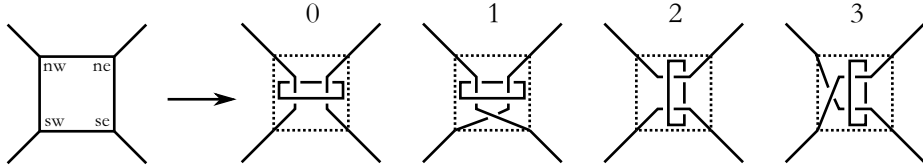


FIGURE 4. Fill tangle.

We drew in Figure 5 the link that corresponds to the sequence 021213 as an example.

Since performing surgery on an augmented circle with slope $-1/p$ (resp. $1/p$) corresponds adding positive (resp. negative) p full twist to the knot components

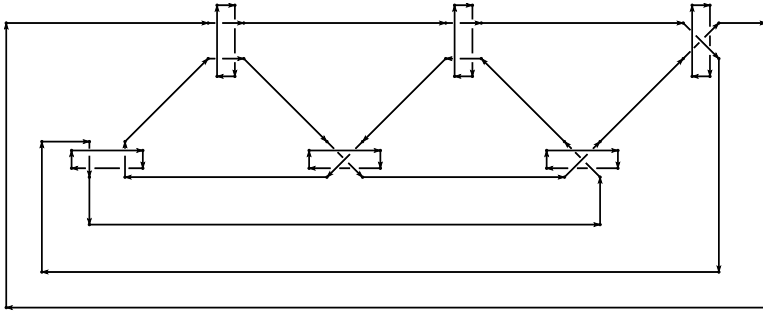


FIGURE 5. The link corresponding to 021213.

running through the augmented circle, by varying the signs and p , we can enumerate all links with diagrams we must consider. However, first we enumerate the augmented links by associating each link to a sequence $\{a_i\}_{i=0}^{l-1}$, where l is the number of augmented circles. We define a *knot component* as a component of the link which is not an augmented circle.

5.2. Conditions. We now describe conditions which will reduce the number of sequences we need to consider.

5.2.1. Alternating knots and Twist number. Since we are only interested in *alternating knots*, we have some constraints. First, we only need to deal with sequences whose corresponding links have one connected knot component, for otherwise after twisting we get a link rather than a knot.

Condition 1. We only consider sequences, each of whose related link has one connected knot component.

Given an alternating diagram the mirror image of the diagram will also be alternating. Therefore after fixing the sign of the surgery slopes along the augmented circles, we may assume that the sign on the 0-th component is negative. This reduces the number of cases we need to consider by a factor of two. We thus obtained the following conditions on slopes.

Condition 2. For the link which is related to a sequence $\{a_i\}_{i=0}^{l-1}$, we consider the following conditions on surgery slopes;

- the slope of the augmented circle in 0-th square is $-1/p_0$ for some $p_0 > 0$,
- the slopes of the other augmented circles are of type $1/p_i$ with $p_i \neq 0$, and their signs are determined so that the resulting knot is alternating.

We will only consider surgeries along slopes satisfying Condition 2.

Remark 3. There was an ambiguity of the sign of crossings when $a_i \equiv 1 \pmod{2}$. We choose the sign of such crossings so that we only need to look at slopes $1/p$ or $-1/p$ with p ranging all positive integers.

Thus we generate a list of links with information of the number of augmented circles on which we perform surgery with negative slope, i.e. $-1/p$'s with positive p . This number is equal to the number of positive twists of the resulting alternating knots. For each link in the list we have generated, the 0-th component is the

knot component, 1-st to i -th components are the augmented circles which will be surgered with negative slopes, and the rest will be surgered with positive slopes.

For the case of 7 and 8 twists, equivalently, the case of length 7 and 8 sequences, not only requiring knot component to be connected, we also require that, after twisting, the twist number does not decrease. For example, in the length 7 case, we require either $a_0 \in \{2, 3\}$ or $a_6 \in \{2, 3\}$. For otherwise, it can readily be seen that any resulting knot after twisting has at most 6 twists. We have similar conditions for the length 8 cases. This occurs if there are *parallel* augmented circles. Here augmented circles are said to be parallel if they are mutually isotopic in the complement of knot component. Thus we have the following condition.

Condition 3. The link which is related to a sequence $\{a_i\}_{i=0}^{l-1}$ has no pair of parallel augmented circles.

5.2.2. *Symmetry.* Next we use symmetries of the plane graph $G_6, G_7, G_8^s, G_8^1, \dots, G_8^6$ to reduce the number of sequences to consider.

We first discuss the graph G_6 , which corresponds to the 6 twists case. For the remainder of this section, we will denote a symmetry by its permutation on the set of tangle regions and when necessary add or subtract a number of twists. For example, the symmetries of the graph G_6 are as follows:

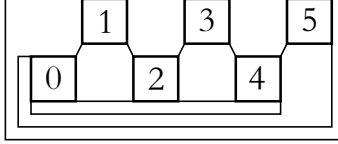


FIGURE 6. The regular 4-valent simple plane graph with 6 vertices.

- $a_0 a_1 a_2 a_3 a_4 a_5 \mapsto a_1 a_2 a_3 a_4 a_5 a_0$,
- $a_0 a_1 a_2 a_3 a_4 a_5 \mapsto a_5 a_4 a_3 a_2 a_1 a_0$.

These symmetries are good enough to reduce the number of sequences in the list and are easy to implement. We implement the above procedure as `twistLink6.py` and by running it, we get a list with 185 links.

Next we consider the graph G_7 (Figure 7).

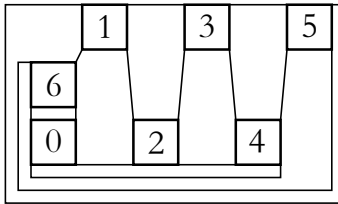


FIGURE 7. The graph G_7 for 7 twists.

We will use the following symmetries. Here each element should be in $\{0, 1, 2, 3\}$ and hence when we add 2, it will be modulo 4. Note that the symmetries we used here are the vertical bilateral symmetry and a π -rotation, see Figure 8.

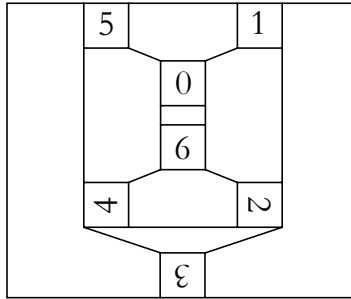


FIGURE 8. G_7 has two bilateral symmetries.

- $a_0 a_1 a_2 a_3 a_4 a_5 a_6 \mapsto a_6 (a_2 + 2)(a_1 + 2) a_3 (a_5 + 2)(a_4 + 2) a_0$,
- $a_0 a_1 a_2 a_3 a_4 a_5 a_6 \mapsto a_6 (a_4 + 2)(a_5 + 2) a_3 (a_1 + 2)(a_2 + 2) a_0$.

Finally we consider the graphs with 8 vertices. As shown in Lemma 4.2, we need to consider two types of graphs; The unique simple plane graph G_8^s (see Figure 9), and G_8^i 's. See Figure 10, 11, 12, 13, 14, and 15 for pictures and symmetries of G_8^i 's.

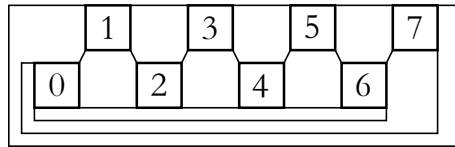


FIGURE 9. The regular 4-valent simple planar graph with 8 vertices.

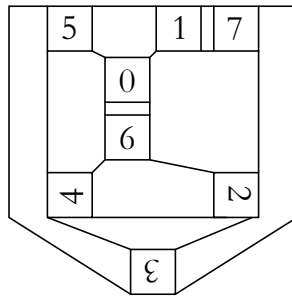


FIGURE 10. G_8^1 .

We now summarize the symmetry which is depicted in the figures in terms of sequences. Note that G_8^3 , G_8^4 , G_8^5 , and G_8^6 have bilateral symmetries and the symmetries following the mark “*” are those corresponding to bilateral symmetries. As we did for 7 twists case, the addition here is modulo 4.

- (1) G_8^s
 - $a_0 a_1 a_2 a_3 a_4 a_5 a_6 a_7 \mapsto a_1 a_2 a_3 a_4 a_5 a_6 a_7 a_0$,
 - $a_0 a_1 a_2 a_3 a_4 a_5 a_6 a_7 \mapsto a_7 a_6 a_5 a_4 a_3 a_2 a_1 a_0$.
 - * $a_0 a_1 a_2 a_3 a_4 a_5 a_6 a_7 \mapsto a_6 a_5 a_4 a_3 a_2 a_1 a_0 a_7$.

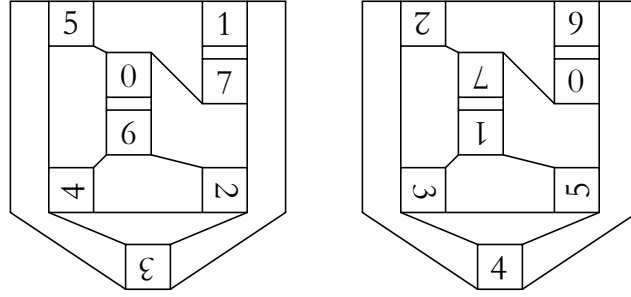


FIGURE 11. G_8^2 (left) and the image under the action of its symmetry (right).

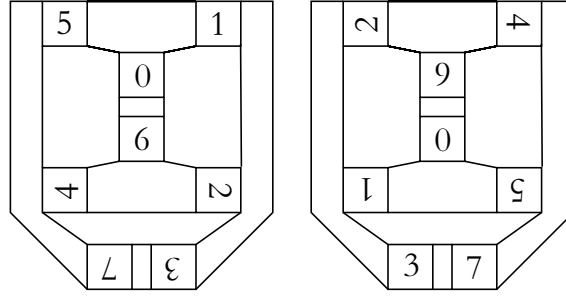


FIGURE 12. G_8^3 (left) and the image under the action of its symmetry (right).

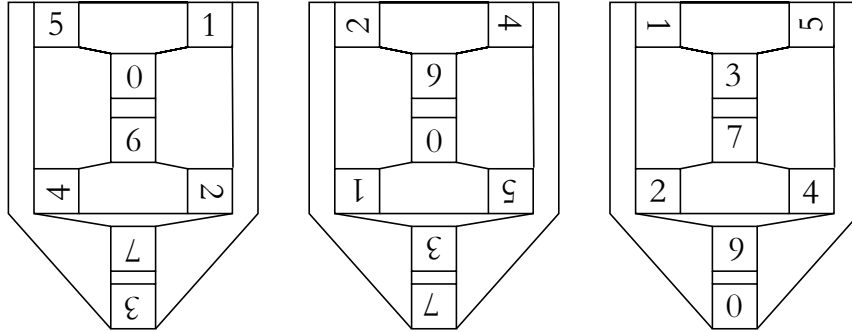
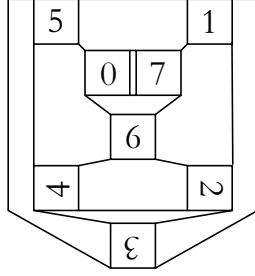
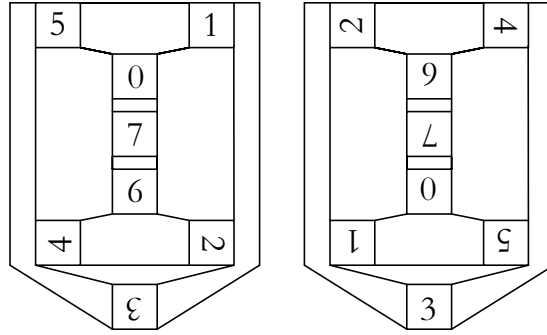


FIGURE 13. G_8^4 (left) and the images under the action of its symmetry (middle) and (right).

- * $a_0 a_1 a_2 a_3 a_4 a_5 a_6 a_7 \mapsto a_0 a_7 a_6 a_5 a_4 a_3 a_2 a_1$.
- (2) G_8^1
- No symmetry.
- (3) G_8^2
- $a_0 a_1 a_2 a_3 a_4 a_5 a_6 a_7 \mapsto a_7 a_6 a_5 a_4 a_3 a_2 a_1 a_0$.
- (4) G_8^3
- $a_0 a_1 a_2 a_3 a_4 a_5 a_6 a_7 \mapsto a_6(a_4 + 2)(a_5 + 2)a_7(a_1 + 2)(a_2 + 2)a_0 a_3$, and
 - * $a_0 a_1 a_2 a_3 a_4 a_5 a_6 a_7 \mapsto a_0 a_5 a_4 a_7 a_2 a_1 a_6 a_3$.

FIGURE 14. G_8^5 .FIGURE 15. G_8^6 (left) and the image under the action of its symmetry (right)

- (5) G_8^4
- $a_0 a_1 a_2 a_3 a_4 a_5 a_6 a_7 \mapsto a_6(a_4 + 2)(a_5 + 2)a_7(a_1 + 2)(a_2 + 2)a_0 a_3$,
 - $a_0 a_1 a_2 a_3 a_4 a_5 a_6 a_7 \mapsto a_3(a_5 + 2)(a_4 + 2)a_0(a_2 + 2)(a_1 + 2)a_7 a_6$, and
 - * $a_0 a_1 a_2 a_3 a_4 a_5 a_6 a_7 \mapsto a_6(a_2 + 2)(a_1 + 2)a_7(a_5 + 2)(a_4 + 2)a_0 a_3$.
- (6) G_8^5
- * $a_0 a_1 a_2 a_3 a_4 a_5 a_6 a_7 \mapsto a_7 a_5 a_4 a_3 a_2 a_1 a_6 a_0$.
- (7) G_8^6
- $a_0 a_1 a_2 a_3 a_4 a_5 a_6 a_7 \mapsto a_6(a_4 + 2)(a_5 + 2)a_3(a_1 + 2)(a_2 + 2)a_0 a_7$.
 - * $a_0 a_1 a_2 a_3 a_4 a_5 a_6 a_7 \mapsto a_0 a_5 a_4 a_3 a_2 a_1 a_6 a_7$.

5.3. Persistent genuine lamination. Using Conditions 1 and 3 together with symmetries of the graph discussed above, we reduce the number of sequences, equivalently, the number of links we have to consider. However, in the proof of Lemma 4.4, the number of components of the links is crucial on computational time. The following lemma enables us to reduce the number of components for most of the links. This is an application of the result obtained by Wu in [51], which is of interest in its own right.

Lemma 5.1. *Let L_0 be a link corresponding to a sequence satisfying Conditions 1 and 3 for one of the 9 graphs in Figure 1 as explained in §5.1. After assigning an orientation to the knot component of L_0 , suppose that the pair of segments on the knot component passing through an augmented circle A of L_0 are anti-parallel (see Figure 16). If we perform Dehn surgeries on A satisfying Condition 2 other than*

the ones corresponding to single full-twists, then any alternating knot obtained by twisting along the other augmented circles admits no exceptional surgeries, or it has a reduced alternating diagram with twist number less than the number of vertices of the plane graph used to construct L_0 .

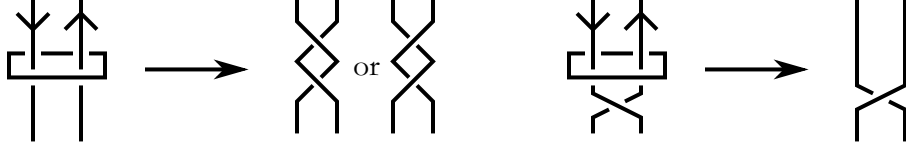


FIGURE 16. Allowable twisting for anti parallel edges.

Remark 4. In Figure 16, only one of the full-twists is shown in the case A has a crossing, namely the one with one crossing remaining, because we just perform Dehn surgeries on A satisfying Condition 2. Please see Remark 3.

Proof of Lemma 5.1. First we show that any Dehn surgeries on the alternating knots which we consider in the lemma yield manifolds containing essential laminations by using the following result obtained by Wu [51, Corollary 6.9]. We here omit the definition and properties of essential laminations. See [51] for details.

Let L be a non-split oriented link, and F a π_1 -injective spanning surface of L . Take an arc α on F , and take a regular neighborhood D of α embedded in F . Set up a coordinate on the boundary of $B = N(\alpha)$ in S^3 so that $L \cap \partial D = a_1 \cup a_2$ gives a 0-tangle and $F \cap \partial B$ is isotopic to a $1/0$ -tangle. Consider the knot K obtained from L by replacing $a_1 \cup a_2$ with a $1/n$ -tangle. Suppose that $|n| > 2$ is odd if α connects parallel arcs, and even otherwise. Here α is said to *connect parallel arcs* (resp. *connect antiparallel arcs*) if the orientations of a_1, a_2 points to the same direction (resp. the different direction). Then, for any non-meridional slope r , the surgered manifold $K(r)$ contains an essential lamination.

We need to check whether it is applicable to our setting. Let k_0 denote the knot component of L_0 . From L_0 , a 2-component link $L_1 = k_0 \cup A$ is obtained by twisting along augmented circles other than A . Here we further require the twisting above satisfies Condition 2. For simplicity, we only consider the case where the surgery slopes for A are $-1/m$ for some $m > 0$.

Let L be the link obtained from L_1 by replacing the tangle corresponding to A with the 0-tangle (without augmented circles). Here we regard the tangle corresponding to A as the $1/0$ - or $-1/1$ -tangle by ignoring A . See Figure 17.



FIGURE 17. Replacement to 0-tangles.

Note that the diagram D of L so obtained must be alternating, and has an orientation induced from that of k_0 . Since any the 9 graphs in Figure 1 has no

cut vertex, D has to be non-split, and so, L is a non-split oriented link by [30]. Let α be the arc connecting the 2 strands of the 0-tangle replaced from the tangle corresponding to A . See Figure 17. Consider the checker-board surface F for the diagram D containing α . Then, by [9, Lemma 2.1], F is a π_1 -injective spanning surface for L if D is a reduced alternating diagram of L .

Assume for the sake of a contradiction that D is not reduced. Then the vertex substituted by the tangle corresponding to A and the vertex corresponding to the reducible crossing in the graph gives a pair of cut vertices. That is, removing the pair of vertices, the graph must become disconnected. Among the 9 graphs in Figure 1, only for the graphs G_7 and G_8^1, \dots, G_8^6 might this arise, and then only if the pair of vertices is the pair adjacent to a bigon. However, such a reducible vertex can appear only if the knot obtained by performing twistings on the augmented circles from L_0 has a reduced alternating diagram with twist number less than the number of vertices of the plane graph used to construct L_0 .

Thus, otherwise, it follows that D is a reduced alternating diagram of L , and F is a π_1 -injective spanning surface for L .

Now we note that performing Dehn surgery on A along the slope $-1/m$ is equivalent to performing replacement $a_1 \cup a_2$ with $1/(2m-1)$ -tangle (resp. $1/(2m)$ -tangle) if α connects parallel arcs (resp. antiparallel arcs). Thus if an alternating knot K is obtained from L_1 by Dehn surgeries on A along the slope $-1/m$, then K is obtained from L_1 by replacing $a_1 \cup a_2$ with the $1/n$ -tangle with $n = 2m - 1$ (resp. $n = 2m$) if α connects parallel arcs (resp. antiparallel arcs).

Consequently, we can apply [51, Corollary 6.9] to the setting above to obtain that, under the assumption of the lemma, for an alternating knot K obtained from L_1 by Dehn surgeries on A along the slope $-1/m$, the surgered manifold $K(r)$ contains an essential lamination for any non-trivial slope r .

Next we show that the laminations in the surgered manifold $K(r)$ so obtained are all *genuine*, i.e., it is carried by an essential branched surface with at least one complementary component which is not an I -bundle. To see this, as claimed in the proof of [51, Corollary 6.9], we note that one of the complementary component of the essential branched surface in $K(r)$ is the same as the exterior of L cut along F . Then, by a work of Adams [1, Theorem 1.9], or its generalization [10, Theorem 1.6], we see that F is not a fiber surface, in particular, the exterior of L cut along F is not an I -bundle. Thus the laminations in the surgered manifold $K(r)$ so obtained are all genuine.

This implies that the surgered manifold $K(r)$ is not a small Seifert fibered space due to the result by Brittenham [6]. Suppose that some Dehn surgery on the alternating knot which we consider in the lemma yields a non-hyperbolic manifold. Then, as explained in the proof of Corollary 1.2, it is already known that the manifold must be irreducible, since any hyperbolic alternating knot has no reducible surgeries. If the manifold is toroidal, then, also as explained in the proof of Corollary 1.2, it is known that the knot must admit a reduced alternating diagram with twist number at most three, less than the number of vertices of the plane graph used to construct L_0 . Thus it suffice to consider the case that the surgered manifold is small Seifert fibered. Thus the proof of the lemma is completed. \square

By Lemma 5.1, we can perform twisting along some augmented circles beforehand with slope $1/1$ or $-1/1$. This reduces the number of components of the links.

Furthermore, by this twisting, the twist number may decrease, see Figure 18. In this case, we do not need to investigate the link. Thus we can reduce the number of links to investigate as well. Thus it gives an additional condition.

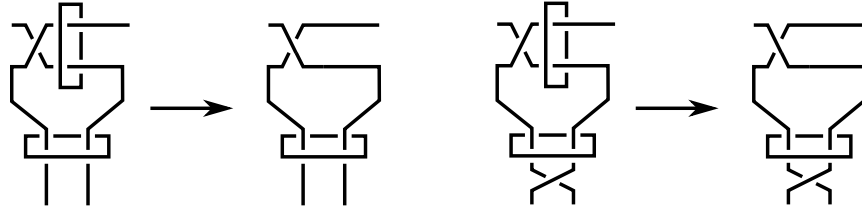


FIGURE 18. The number of twists will decrease.

5.4. **Code.** The whole procedure, namely generating links and applying symmetry and Lemma 5.1, is implemented as a set of files `twistLink.py`'s.

Here, in the case of 7 twists, we summarize the code `twistLink7.py` in Algorithm 1. We can check if a given sequence satisfies Condition 1 by carefully tracing the knot components and checking if it is connected. The code for 6 or 8 twists case works similarly. We note that for each sequence, we first make a `.lnk` file which is a SnapPy's format for links drawn on `plink` and then, read that file on SnapPy to get a triangulation of the link complement. We perform Dehn surgery if we can apply Lemma 5.1 and as a result we save a `.tri` file that is a SnapPea's format for a triangulation. For `.lnk` and `.tri` files, see the documentation of SnapPy [8].

In Table 1, we summarized the number of links that we obtained by running the code.

TABLE 1. Number of links

Graph	number of links
G_6	185
G_7	1271
G_8^s	2171
G_8^1	11299
G_8^2	5503
G_8^3	2645
G_8^4	1651
G_8^5	3004
G_8^6	2675
Total	30404

Consequently we have proved Lemma 4.3.

6. PROCEDURES FOR COMPUTER-AIDED CALCULATIONS

In this section, we give detailed explanations on our code `fef.py`, and give a proof of Lemma 4.4 established by computer-aided calculations using the code.

Algorithm 1 Enumerating augmented links

Input: Graph G_7 .**Output:** Triangulation files of 1271 link complements.

Prepare a list, named checked.

for a sequence $\{a_i\}_{i=0}^6$ of $\{0, 1, 2, 3\}$ of length 7 **do**Check if $\{a_i\}_{i=0}^6$ is in is_checked file. If it is, we go to the next sequence.**if** $\{a_i\}_{i=0}^6$ satisfies Conditions 1 and 3 **then**

Add symmetric sequences

- $a_6(a_2 + 2)(a_1 + 2)a_3(a_5 + 2)(a_4 + 2)a_0$,
- $a_6(a_4 + 2)(a_5 + 2)a_3(a_1 + 2)(a_2 + 2)a_0$.

in checked list.

Draw edges of G_6 depicted in Figure 6.Determine the sign of the crossings in the rectangles if any and the number n of slopes that will be surgered with negative slopes. (see explanation in §5.2.)Fill rectangles according to $\{a_i\}_{i=0}^6$ (Figure 4). {So far, we are dealing with .lnk file.}**for** $0 \leq j \leq 6$ **do****if** Two edges passing through the augmented circle in j -th rectangle are anti-parallel (Figure 16) **then**Perform a surgery on the augmented circle in j -th rectangle along the slope $1/1$ or $-1/1$. {Applying Lemma 5.1. Here we use .tri file. We choose the sign so that Condition 2 is satisfied.}**if** After the surgery, the number of twists decrease (Figure 18) **then**

Skip this sequence and go to next sequence.

end if**end if****end for**

Save the resulting triangulation file.

end if**end for**

6.1. A discussion of the code. We here explain some features of our code `fef.py`.

This is based on the code developed in [26]. In [26], using the code, the authors gave a complete classification of exceptional fillings of the minimally twisted five-chain link complement, a well-known hyperbolic link of 5 components in S^3 . However we had to modify the code, since the code in [26] essentially depends upon the code given in [33]. To obtain mathematically rigorous computations that cooperate well with the program we improved their code using verified numerical analysis based on interval arithmetic. Some fundamentals about such method will be given in Appendix A. Note that the key step to show the links have no exceptional surgeries heavily depends upon the techniques developed in [13] by the team containing the authors of this paper.

The main algorithm of [13] returns not only a certificate of hyperbolicity for a given triangulated manifold M , but also closed sets in \mathbb{C} that contain the exact tetrahedral shapes. The methods of that paper use interval arithmetic to establish this claim. While technically the shapes are in a (real valued) interval cross (real

valued) interval, i.e. a rectangular box, we will slightly abuse notation and say that each tetrahedral parameter is determined up to an interval. As noted in [13], one of the advantages of interval arithmetic is that it naturally extends to the computations of other invariants and geometric data of the manifold M .

One such piece of geometric data is *parabolic length*, i.e. given a horoball packing of M that is maximal in the sense that each horoball in the packing is tangent to at least one other horoball, we can define the length of a parabolic element p fixing a horosphere S setwise as the translation displacement of p in S . For a one cusped manifold, this length is canonically defined, however if M has more than one cusp, this quantity will depend on our choice of horoball packing. The 6-Theorem, proved independently by Agol [2] and Lackenby [23], provides a key application of parabolic length to our problem namely if M is filled along a sufficiently long slope r , then the filled manifold $M(r)$ is hyperbolic. If M is filled along multiple cusps by slopes s_1, \dots, s_n , we pay specific attention to [23, Theorem 3.1], which states that filling is hyperbolic provided in some horoball packing each slope, s_i , we fill along has length strictly bigger than 6. In the actual computations, we actually enumerate slopes of length less than 6.0001. Note that even if we use interval arithmetic, we need to compare floating point numbers, which are the ends of intervals, to prove inequality. Here we use 6.0001 instead of 6 because floating point numbers are not designed to be used for equality.

The code `fef.py` enumerates all sets of such slopes for a manifold M . As mentioned above, parts of our code and `fef.py` in particular are very directly adapted from the code explained [26, §2.1] (compare to their `find_exceptional_fillings.py`). Pseudo-code for `fef.py` is provided as Algorithm 2.

As noted above, `fef.py` is based upon the file `find_exceptional_fillings.py` used in the first version of [26]. In the latest version of `find_exceptional_fillings.py`, they integrated our code. Although the old version of `find_exceptional_fillings.py` is not available anymore, we give some explanation to clarify our contribution. For the purposes of the following discussion `fef.py` will be used to denote our file and `find_exceptional_fillings.py` will be used to denote the code used for the first version of [26]. One of the key differences between the two files is that `fef.py` is written to employ interval arithmetic. However, while the significance of this change is seemingly only visible in a few places such as the declarations of variables, it underpins the error control we employ to make the computation rigorous. The two methods also differ in selecting a horoball packing to compute parabolic length. The manifolds we are interested in have a distinguished cusp, namely that corresponding to the knot component, whereas the manifolds in [26] do not. Furthermore, `find_exceptional_fillings.py` and the arguments surrounding its implementation cut down the number of cases by using the symmetries of the minimally twisted five chain link, and so there is a preference toward keeping the horoball packing as symmetric as possible.

To better reduce the number of cases we must consider, we have found it (experimentally) advantageous to choose a horoball packing where the equivalence class of horoballs corresponding to the cusp of the knot component has as much volume as possible so that the slopes in that cusp are as long as possible. Consequently, `fef.py` inflates this horoball past the point of all horoballs being equal volume and reduces the volumes of the other horoballs accordingly. This also produces a horoball packing that is invariant under the symmetries described in §5.2.2, and so

Algorithm 2 The algorithm for `fef.py`

Input: A triangulation T of a manifold N .

Output: A verification that all non-trivial Dehn surgeries of a manifold fitting the conditions of §5.2 are hyperbolic.

Try to canonize T .

if T can be canonized and hikmot verified the hyperbolicity of canonized triangulation. **then**

Use the canonized triangulation.

else if Find a triangulation whose hyperbolicity is checked by hikmot. **then**

Use the found triangulation.

else

If we cannot find any triangulation that hikmot verifies hyperbolicity, we give up. (This didn't happen in our computation for alternating knots)

end if

Compute lower bounds for the cusped areas of N using the (already) verified tetrahedral shapes for T . For each cusp, also compute the cusp shape as a parallelogram determined by a quotient of the complex plane by 1 and $x + yi$. Finally, compute a lower bound for the diameter of the horoball for that cusp and enforce with this bound that the intersection of the boundary of a horoball (not centered at ∞) and an ideal tetrahedron having a vertex at ∞ intersect in a triangle.

if Failed on some procedure above. **then**

Use $\frac{3\sqrt{3}}{8}$ as a lower bound for cusp area (horoball of this size always exists by a standard fact of hyperbolic 3-manifolds, see e.g. Proposition 2 in `cusp_neighborhoods.cc` of Weeks' SnapPea kernel code, available at the webpage of SnapPy [8]). For these cusps, the cusp shape is determined by 1 and $x + yi$ with $x = 0$ and $y = \frac{3\sqrt{3}}{8}$.

end if

The length of a slope $\frac{p}{q}$ is $\sqrt{\frac{A}{y}((p+xq)^2 + (yq)^2)}$, where A is the area of corresponding horosphere. List all slopes of length less than 6.0001 in these cusps. For slopes on each cusp less than length 6.0001, perform surgery with that slope if it meets Condition 2 of §5.2.1.

if All cusps have been surgered along. **then**

Verify that the surgered manifold is hyperbolic.

else

Verify this intermediately surgered manifold is hyperbolic and repeat the procedure above to find all slopes of length less than 6.0001 in the cusps of this partially surgered manifold and (recursively) verify the hyperbolicity of these surgeries.

end if

is very much in the same spirit as symmetry reductions employed in [26]. Furthermore, this optimization appears to be crucial since we are dealing with 30404 links and we want to reduce the number of slopes to compute as far as possible.

6.2. Computation environments and verifying computations. As we have seen in the previous subsection, the code `fef.py` computes recursively with respect to the number of cusps. Usually, for each augmented circle of our links generated as

explained in §5, there are 2 or 3 surgery slopes of parabolic length less than 6. In the worst case, there are about 18,000 manifolds to investigate for a single link. In this case, it takes about 51 hours on a single CPU of TSUBAME (The computational ability of a single CPU of TSUBAME is comparable to that of a standard personal computer). Since there are 30404 links, we need high-spec machine. The second author was able to access "TSUBAME", the super-computer of Tokyo Institute of Technology. See the website [47] of TSUBAME for a basic information, [27] for a brief survey, and [28] for a detailed exposition. Roughly speaking, on TSUBAME, one can use many machines at the same time. Although generally, to use parallel computation effectively we need some work, in our case, the situation itself is totally parallel, that is, we need to investigate each link independently. Thus we can use TSUBAME effectively. In practice, we "rented" 64 machines from TSUBAME, and then it took a week to prove Theorem 1.1.

Proof of Lemma 4.4. Let L be one of the 30404 augmented links in S^3 obtained in Lemma 4.3, and K an alternating knot obtained by a Dehn surgery on L such that the surgery corresponds to twisting along the unknotted components of L . By construction, K has a reduced alternating diagram with twist number at least 6, and so it is not a torus knot of type $(2, p)$. This implies that K is hyperbolic by [30].

We show that K admits no non-trivial exceptional surgeries by running our code `fef.py` on TSUBAME for the triangulation files of the 30404 augmented links obtained by the files `twistLink.py`'s.

On TSUBAME, we need to know a specified command to run it. The command we used is

```
t2sub -q V -J 0-11299 -l walltime=5:00:00 -W group_list=t2gxxx
-l select=1 ./8twist1.sh.
```

Note that the command should be in one line. We here explain this command. First, "t2sub" is the basic command to run TSUBAME and we used several options;

- "-q V" specifying a queue name to submit a job (always necessary).
- "-I walltime = 5:00:00" meaning that if the computation time exceeded 5 hours, then we quit the computation.
- "-W group_list=t2gxxxxxx" specifying the name of the user.
- "-I select= n " meaning that for a single computation (i.e. a single link in our case), we use " n machines", and
- `./8twist1.sh` is the execution file. The contents are as follows;


```
#!/bin/sh
cd ${PBS_O_WORKDIR}
python fef.py 8twist1tri/dataname${PBS_ARRAY_INDEX}.tri
Here $PBS_O_WORKDIR is the current directly and,
```
- "-J 0-11299" means that `$PBS_ARRAY_INDEX` ranges from 0 to 11299.

We remark here although `twistLink.py`'s generate the triangulation files named like `0.021213.tri`, (here the first 0 is the number of augmented circles that will be filled with $1/p$ with negative p) we renamed all the triangulation files to "`datanamen.tri`" so that it will be suitable for "-J" option above, called array job. The information about the number of augmented circles that will be filled with negative slopes are stored in the contents of the files.

TSUBAME returns an outputs file and an error file for each triangulation file.
We here include examples,

- output file


```
8twist1tri/dataname1015.tri
./4_20320113.lnk_filled(0,0)(0,0)(0,0)(0,0)
Manifold volume:
31.5182982095
Cusp shapes:
Cusp 0 : complete torus cusp of shape (5.02637698521+9.96657568374j),
Cusp 1 : complete torus cusp of shape (0.594148461042+0.999088628226j),
Cusp 2 : complete torus cusp of shape (0.333034596342+1.15348583079j),
Cusp 3 : complete torus cusp of shape (0.333034596342+1.15348583079j)
With 4 fillings:
Total: 0
Candidate hyperbolic fillings:
With 4 fillings:
[]
Total: 0
8twist1tri/dataname1015.tri done
Computer time needed: 0:00:16.603389
Number of manifolds hikmot ensured the hyperbolicity 19
```
- error file


```
=====
Your accounting ID
group id : t2xxxxxxx
-----
Job informations
job id : 60373[1015].t2zpbs-vm1
queue : V
num of used node(s) : 1
used node(s) list :
t2a001137-vm1
used cpu(s) : 1
walltime : 00:00:16 (16 sec)
used memory : 26080kb
job exit status : 0
-----
Accounting factors
x 1.0 by queue
x 1.0 by job priority
x 1.0 by job walltime extension
= 1.0 is the total accounting factor
-----
Expense informations
maximum CPU units with factors : 64
used CPU units : 1
```

=====

This proves the link obtained from G_8^1 and the sequence 20320113 does not have any exceptional surgeries satisfying Condition 2. By running `fef.py` on TSUBAME, we have 30404 output files and error files.² These data are available at [20]. The versions of gcc and python, and any other relevant information on the nodes of TSUBAME that we used are shown in Table 2. Fortunately, for all 30404 manifolds, the outputs show that they have no exceptional surgeries satisfying Condition 2. In total, i.e. the sum of the computation time of all nodes, computation time was approximately 512 days, and the number of manifolds we applied hikmot is 5646646. Consequently we have completed our proof of the Lemma 4.4. \square

TABLE 2. A description of the computer system used for this computation

SnapPy	snappy-1.3.12-py2.6-linux-x86_64.egg
HIKMOT	HIKMOT_ver0.1.0
FEF	fef_ver1.1
PYTHON	python2.6
TSUBAME(version 2) :	
OS	SUSE Linux Enterprise Server 11 SP3
Job Scheduler	PBS Professional
Compilers	Intel Compiler 2013.1.046 (default), PGI CDK 14.6, gcc 4.3.4
MPI	OpenMPI 1.6.5 (default), MVAPICH2 2.0rc-1
CUDA	6.0.1
CUDA driver	331.62

ACKNOWLEDGEMENTS

The authors would like to thank Neil Hoffman, Bruno Martelli, Nathan Dunfield, and Marc Culler for helpful discussions. They also thank the Support team of TSUBAME for providing technical support, and Shin'ichi Oishi, Masahide Kashiwagi, and Akitoshi Takayasu for their help with the building the verification tools needed to implement this project. They would also like to thank Matthias Goerner for catching a bug in the earlier version of our program. Finally they thank the referees for their careful readings and useful comments.

APPENDIX A. VERIFIED COMPUTATION

In this section, we recall briefly the notion of *interval arithmetic*, that makes it possible to prove rigorously inequality by using computer. In `fef.py`, we use so-called 6-Theorem, that states that if a parabolic length of a slope is greater than 6, then the surgery along that slope gives a hyperbolic manifold. Hence to study

²Unfortunately the version 1.1 of `fef.py` contained a small bug, which could be immediately fixed in the update version (`fef_ver1.4`). It was not relevant to the main procedure, but for rigorousness, we have performed re-computation, and obtained the same outcomes (in February, 2016). Please see the readme file of `fef.py` available on our web site [20].

exceptional surgeries, we only need to consider slopes of length less than 6, and here we need to prove inequality.

On usual computation, we use *floating point arithmetic*. The floating point arithmetic is a very practical method to perform approximated computation. Here we do not go into detail, instead let us note that the set $\mathbb{F} \subset \mathbb{R}$ of real numbers that can be represented by floating point arithmetic satisfies $|\mathbb{F}| < \infty$. There are several ways to define $r : \mathbb{R} \rightarrow \mathbb{F}$, which is called a rounding operator. Here we would have some error that might accumulate by iterating this process. Interval arithmetic is introduced to deal with this unpleasant error [43, 44, 32]. In interval arithmetic, instead of dealing with approximated values, we use closed intervals of type $X = [\underline{x}, \bar{x}]$. We denote the set of all intervals by \mathbb{IR} . We will design our computation as follows so that each of our intervals contains the exact value. We first recall abstract theory of interval arithmetic and later, we will explain so-called machine interval arithmetic. First, for a given function $f : \mathbb{R} \rightarrow \mathbb{R}$, a function $F : \mathbb{IR} \rightarrow \mathbb{IR}$ is said to be an interval extension of f if

$$F(X) \supset \{f(x) \mid x \in X\}, \forall X \in \mathbb{IR}.$$

We remark here that in `fef.py`, the only function we use is the square root, a monotone function. Hence in practice we only need to consider endpoints of a given interval. We further define interval extensions of four arithmetic operations as follows;

$$\begin{aligned} X + Y &= [\underline{x} + \underline{y}, \bar{x} + \bar{y}], \\ X - Y &= [\underline{x} - \bar{y}, \bar{x} - \underline{y}], \\ X \cdot Y &= [\min\{\underline{x} \cdot \underline{y}, \bar{x} \cdot \bar{y}, \underline{x} \cdot \bar{y}, \bar{x} \cdot \underline{y}\}, \max\{\underline{x} \cdot \underline{y}, \bar{x} \cdot \bar{y}, \underline{x} \cdot \bar{y}, \bar{x} \cdot \underline{y}\}], \text{ and} \\ X/Y &= X \cdot \left[\frac{1}{\bar{y}}, \frac{1}{\underline{y}}\right], \quad (0 \notin Y). \end{aligned}$$

To implement the interval arithmetic we need to consider \mathbb{IF} , the set of closed intervals whose endpoints are elements of \mathbb{F} . We define two rounding operators $\lceil \cdot \rceil_{\mathbb{F}}, \lfloor \cdot \rfloor_{\mathbb{F}} : \mathbb{R} \rightarrow \mathbb{F}$ as

$$\lceil x \rceil_{\mathbb{F}} = \min\{y \in \mathbb{F} \mid x \leq y\}, \quad \lfloor x \rfloor_{\mathbb{F}} = \max\{y \in \mathbb{F} \mid x \geq y\}.$$

Then we can define a rounding operator $\square : \mathbb{IR} \rightarrow \mathbb{IF}$ as $\square([\underline{x}, \bar{x}]) = [\lfloor \underline{x} \rfloor_{\mathbb{F}}, \lceil \bar{x} \rceil_{\mathbb{F}}]$. Then for a given interval extension F of f , we define the machine interval extension $\bar{F} : \mathbb{IR} \rightarrow \mathbb{IF}$ of F by $\bar{F}(X) = \square(F(X))$. Similarly for $\circ \in \{+, -, \times, /\}$, the machine interval extension is defined as $X \circ Y = \square(X \circ Y)$. Thus we can handle round off errors. If we use machine interval arithmetic, it can be readily seen that the exact value is always contained in the interval that we compute. Therefore we can rigorously prove inequality by comparing suitable endpoints of resulting intervals. This enables us to prove inequality by computer.

APPENDIX B. A FAMILY OF MONTESINOS KNOTS

We here include an application of our method to obtain a complete classification of exceptional surgeries on the Montesinos knots $M(-1/2, 2/5, 1/(2q+1))$ with $q \geq 5$. Consequently the Montesinos knots are shown to have no non-trivial exceptional surgeries. This gives the last piece for a complete classification of exceptional surgeries on hyperbolic arborescent knots in S^3 .

Let us apply the code `fef_mon.py` (also available at [20]) to the link L_M depicted in Figure 19 (left). The code `fef_mon.py` is essentially the same as `fef.py`, but it is suitably tuned for investigating L_M . It requires two input, namely the name of

the manifold and the number of augmented circles that will be surgered along $1/p$ with $p < 0$, while `fef.py` automatically reads such number from the `.tri` files we generated by `twistLink.py`'s.

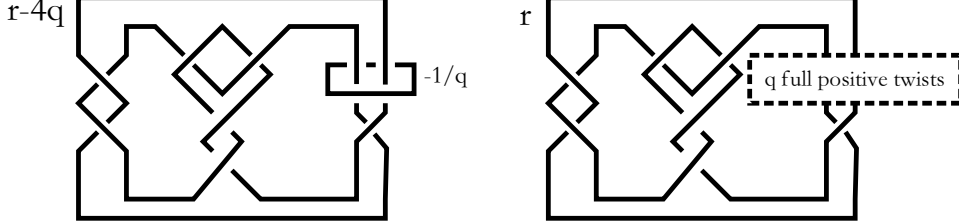


FIGURE 19. (left) L_M , (right) $M(-1/2, 2/5, 1/(2q+1))$.

Remark 5. Since the linking number of the two components of L_M is 2, if we perform Dehn surgery on the augmented circle of L_M , the surgery slope will be twisted. For this reason, for Dehn surgery on $M(-1/2, 2/5, 1/(2q+1))$ with slope r , the corresponding slope on L_M will be $r - 4q$. See [40] for details.

The augmented circle will be filled by slope $-1/q$ and the other component will be filled by slope r . By our code, we see that L_M does not admits any exceptional surgeries with $q > 5$. The output is available in our web site [20].

Although our code can enumerate all exceptional surgeries, for the case of L_M , the list that our code returns contains many redundant, i.e. hyperbolic surgeries. Hence we will apply our code for the case of $q = 1, 2, 3, 4$, and 5 separately by directly drawing diagrams. We summarize the result in Table 3.

TABLE 3. Exceptional fillings

q	r , candidate exceptional	r , candidate hyperbolic
1	3,4,5,6	7
2	7,8,9	6, 10
3	11,12	10,13
4	15	14,16
5	\emptyset	18,19,20

The candidate exceptional fillings in Table 3 are all known to be exceptional. In fact, $K(r)$ is toroidal if $(q, r) = (1, 6), (2, 9), (3, 12), (4, 15)$. See [49, Theorem 1.1]. Otherwise $K(r)$ is small Seifert fibered. See [52, Theorem 3.2], and also see [29]. (Recall that Montesinos knots have no toroidal Seifert fibered surgeries [18].)

Hence to complete the classification, it suffices to prove that all candidate hyperbolic fillings in Table 3 actually give hyperbolic manifold. We will use the following algorithm that we used in [13] to verify the hyperbolicity of Hodgson-Weeks Closed Census [12]. The main idea of Algorithm 3 is due to Craig Hodgson. The code `makepositive_drill.py` available at [20] implements the algorithm. Then by using the code, we can verify the hyperbolicity of all resulting manifolds of candidate hyperbolic fillings. Thus we complete the classification of exceptional surgeries along Montesinos knots.

Algorithm 3 Find positive solutions by drilling out

Input: M is a closed manifold with a surgery description.

Output: M has a good triangulation.

while We could find a short closed geodesic $\gamma \subset M$ **do**

 Drill out γ to get $M \setminus \gamma$,

 Take filled triangulation N of $M \setminus \gamma$,

 Fill the cusp of N by the slope $(1, 0)$.

 (By the above procedure, we forget original surgery description and get new surgery description.)

if N has positively oriented solution. **then**

if hikmot [14] verifies the hyperbolicity of N **then**

 return [True, N]

end if

end if

end while

return False.

This gives the last piece for a complete classification of exceptional surgeries on hyperbolic arborescent knots in S^3 as follows. Any hyperbolic arborescent knot of type III has no exceptional surgeries as shown by Wu [48, Theorem 3.6]. A complete classification of exceptional surgeries on hyperbolic arborescent knot of type II is obtained also by Wu [50]. There are just 3 knots among them admitting exceptional surgeries, which are all toroidal. Hyperbolic type I arborescent knots are two-bridge knots and Montesinos knots of length three. For two-bridge knots, a complete classification of exceptional surgeries is obtained by Brittenham and Wu [7]. The remaining case, for Montesinos knots of length three, other than $M(-1/2, 2/5, 1/(2q+1))$ with $q \geq 5$, a complete classification of exceptional surgeries is recently established by Meier [29]. Now we have shown that $M(-1/2, 2/5, 1/(2q+1))$ with $q \geq 5$ have no exceptional surgeries.

We here include a summary. See [17], [18], [29], [48], [49], [50], [51], [52] for details.

Let K be a hyperbolic arborescent knot in S^3 . Suppose that the manifold $K(r)$ obtained by Dehn surgery on K along a non-trivial slope r is non-hyperbolic for some rational number r . Then r must be an integer except for $r = 37/2$ for $P(-2, 3, 7)$. The manifold $K(r)$ is always irreducible, and has infinite fundamental group except for $r = 17, 18, 19$ for $P(-2, 3, 7)$ and $r = 22, 23$ for $P(-2, 3, 9)$. Furthermore the following hold. If $K(r)$ is toroidal, then $K(r)$ is not a Seifert fibered, and K is either

- a two bridge knot $K_{[b_1, b_2]}$ with $|b_1|, |b_2| > 2$, and $r = 0$ if both b_1, b_2 are even, $r = 2b_2$ if b_1 is odd and b_2 is even,
- a twist knot $K_{[2n, \pm 2]}$ with $|n| > 1$ and $r = 0, \mp 4$,
- one of the Montesinos knots of length 3 with the slope described in Table 4.
- K_1 with $r = 3$, K_2 with $r = 0$ or K_3 with $r = -3$. Here K_1, K_2, K_3 are defined as follows. Let $T(r_1, r_2)$ be the Montesinos tangle obtained as the sum of rational tangles corresponding to r_1 and r_2 . Denote by $T(r_1, r_2; n)$ the tangle obtained from $T(r_1, r_2)$ by twisting the two lower

TABLE 4. Toroidal surgeries

K	r
$P(q_1, q_2, q_3)$, q_i odd and $ q_i > 1$	0
$P(q_1, q_2, q_3)$, q_1 even, q_2, q_3 odd and $ q_i > 1$	$2(q_2 + q_3)$
$P(-2, 3, 7)$	$37/2$
$P(-3, 3, 7)$	1
$M(-1/2, 1/3, 1/(3 + 1/n))$, n even and $n \neq 0$	$2 - 2n$
$M(-1/2, 1/3, 1/(5 + 1/n))$, n even and $n \neq 0$	$1 - 2n$
$M(-1/2, 1/3, 1/(6 + 1/n))$, $n \neq 0$, -1 odd (resp. even)	16 (resp. 0)
$M(-1/2, 1/5, 1/(3 + 1/n))$, n even and $n \neq 0$	$5 - 2n$
$M(-1/2, 2/5, 1/7)$	12
$M(-1/2, 2/5, 1/9)$	15
$M(-1/3, -1/(3 + 1/n), 2/3)$, $n \neq 0$, -1 odd (resp. even)	-12 (resp. 4)
$M(-2/3, 1/3, 1/4)$	13
$M(-1/(2 + 1/n), 1/3, 1/3)$, n odd and $n \neq -1$	$2n$

endpoints of the strands by n left hand half twists. Let $\eta : \mathbb{R}^2 \rightarrow \mathbb{R}^2$ be the map which is a $\pi/2$ counter-clockwise rotation about the origin followed by a reflection along the y -axis. Define three knots K_1, K_2, K_3 obtained as $(S^3, K_1) = T(1/3, -1/2; 4) \cup_\eta T(1/3, -1/2; 4)$, $(S^3, K_2) = T(1/3, -1/2; 4) \cup_\eta T(-1/3, 1/2; -4)$, and $(S^3, K_3) = T(-1/3, 1/2; -4) \cup_\eta T(-1/3, 1/2; -4)$.

If $K(r)$ is small Seifert fibered, then K is either

- the figure-eight knot and $r = \pm 1, \pm 2, \pm 3$,
- a twist knot $K_{[2n, \pm 2]}$ with $|n| > 1$ and $r = \mp 1, \mp 2, \mp 3$,
- one of the Montesinos knots of length 3 with the slope described in Table 5.

TABLE 5. Seifert fibered surgeries

K	r
$P(-2, 3, 2n + 1)$, $n \neq 0, 1, 2$	$4n + 6, 4n + 7$
$P(-2, 3, 7)$	17
$P(-3, 3, 3)$	1
$P(-3, 3, 4)$	1
$P(-3, 3, 5)$	1
$P(-3, 3, 6)$	1
$M(-1/2, 1/3, 2/5)$	3, 4, 5
$M(-1/2, 1/3, 2/7)$	$-1, 0, 1$
$M(-1/2, 1/3, 2/9)$	2, 3, 4
$M(-1/2, 1/3, 2/11)$	$-1, -2$
$M(-1/2, 1/5, 2/5)$	7, 8
$M(-1/2, 1/7, 2/5)$	11
$M(-2/3, 1/3, 2/5)$	-5

REFERENCES

- [1] C. Adams, *Noncompact Fuchsian and quasi-Fuchsian surfaces in hyperbolic 3-manifolds*, *Algebr. Geom. Topol.*, **7**, 565–582, (2007).
- [2] I. Agol, *Bounds on exceptional Dehn filling*, *Geom. Topol.*, **4**, 431–449, (2000).
- [3] S. Boyer and X. Zhang, *Cyclic surgery and boundary slopes*, *Geometric topology* (Athens, GA, 1993), 62–79, *AMS/IP Stud. Adv. Math.*, 2.1, Amer. Math. Soc., Providence, RI, (1997).
- [4] G. Brinkmann, S. Greenberg, C. Greenhill, B.D. McKay, R. Thomas, and P. Wollan, *Generation of simple quadrangulations of the sphere*, *Discrete Math.*, **305**(1-3), 33–54 (2005).
- [5] G. Brinkmann and B.D. McKay, *plantri* (software), available at <http://cs.anu.edu.au/~bdm/plantri>.
- [6] M. Brittenham, *Essential laminations in Seifert-fibered spaces*, *Topology*, **32**(1), 61–85 (1993).
- [7] M. Brittenham and Y.-Q. Wu, *The classification of Dehn surgery on 2-bridge knots*, *Comm. Anal. Geom.*, **9**, 97–113, (2001).
- [8] M. Culler, N. M. Dunfield, and J. R. Weeks. *SnapPy*, a computer program for studying the geometry and topology of 3-manifolds, available at <http://snappy.computop.org>.
- [9] C. Delman and R. Roberts, *Alternating knots satisfy strong property P*, *Comm. Math. Helv.*, **74**, 376–397, (1999).
- [10] D. Futer, E. Kalfagianni, and J. S. Purcell, *Quasifuchsian state surfaces*, *Trans. Amer. Math. Soc.*, **366**(8), 4323–4343, (2014).
- [11] A. Hatcher and W. Thurston, *Incompressible surfaces in 2-bridge knot complements*, *Inventiones Math.*, **79**, 225–246, (1985).
- [12] C. Hodgson and J. Weeks, *Symmetries, isometries and length spectra of closed hyperbolic three-manifolds*, *Experiment. Math.*, **3**, 261–274, (1994).
- [13] N. Hoffman, K. Ichihara, M. Kashiwagi, H. Masai, S. Oishi, and A. Takayasu, *Verified computations for hyperbolic 3-manifolds*, *Experiment. Math.*, **25**, 66–78, (2016).
- [14] N. Hoffman, K. Ichihara, M. Kashiwagi, H. Masai, S. Oishi, and A. Takayasu, *hikmot*, a computer program for Verified computations for hyperbolic 3-manifolds, available at <http://www.oishi.info.waseda.ac.jp/~takayasu/hikmot/>.
- [15] K. Ichihara, *Integral non-hyperbolike surgeries*, *J. Knot Theory Ramifications*, **17**(3), 257–261, (2008).
- [16] K. Ichihara, *All exceptional surgeries on alternating knots are integral surgeries*, *Algebr. Geom. Topol.*, **8**, 2161–2173, (2008).
- [17] K. Ichihara and In Dae Jong, *Cyclic and finite surgeries on Montesinos knots*, *Algebr. Geom. Topol.*, **9**, 731–742, (2009).
- [18] K. Ichihara and I. D. Jong, *Toroidal Seifert fibered surgeries on alternating knots*, *Proc. Japan Acad. Ser. A Math. Sci.*, **90**(3), 54–56, (2014).
- [19] K. Ichihara, I. D. Jong, and Y. Kabaya, *Exceptional surgeries on $(-2, p, p)$ -pretzel knots*, *Topology Appl.*, **159**(4), 1064–1073, (2012).
- [20] K. Ichihara and H. Masai, *fef.py and twistlink.py's*, available at https://researchmap.jp/read0212632/published_papers/17989468?lang=en.
- [21] L. H. Kauffman, *State models and the Jones polynomial*, *Topology*, **26**(3), 395–407, (1987).
- [22] Rob Kirby ed., *Problems in low-dimensional topology*, *AMS/IP Stud. Adv. Math.*, 2.2, *Geometric topology* (Athens, GA, 1993), 35–473, Amer. Math. Soc., Providence, RI (1997).
- [23] M. Lackenby, *Word hyperbolic Dehn surgery*, *Invent. Math.*, **140**(2), 243–282, (2000).
- [24] M. Lackenby and R. Meyerhoff, *The maximal number of exceptional Dehn surgeries*, *Invent. Math.*, **191**(2), 341–382, (2013).
- [25] W. B. R. Lickorish and M. B. Thistlethwaite, *Some links with non-trivial polynomials and their crossing-numbers*, *Comment. Math. Helvetici*, **63**, 527–539, (1988).
- [26] B. Martelli, C. Petronio, and F. Roukema, *Exceptional Dehn surgery on the minimally twisted five-chain link*, *Comm. Anal. Geom.*, **22**, 689–735, (2014).
- [27] S. Matsuoka, T. Endo, N. Maruyama, H. Sato, and S. Takizawa, *The Total Picture of TSUB-AME2.0*, *The TSUBAME E-Science Journal*, Tokyo Tech. GSIC, Vol. 1, pp. 16-18, (2010).
- [28] S. Matsuoka, T. Aoki, T. Endo, H. Sato, S. Takizawa, A. Nomura, and K. Sato, *TSUB-AME2.0: The First Petascale Supercomputer in Japan and the Greatest Production in the World*, *Contemporary High Performance Computing: From Petascale toward Exascale* Edited by Jeffrey S. Vetter, Chapman & Hall/CRC, Chapter 20. pp. 525–556 (2013).

- [29] J. Meier, *Small Seifert fibered surgery on hyperbolic pretzel knots*, *Algebr. Geom. Topol.*, **14**, 439–487, (2014).
- [30] W. Menasco, *Closed incompressible surfaces in alternating knot and link complements*, *Topology*, **23**, 37–44, (1984).
- [31] W. Menasco and M. Thistlethwaite, *Surfaces with boundary in alternating knot exteriors*, *J. Reine Angew. Math.*, **426**, 47–65, (1992).
- [32] R. E. Moore, *Interval Analysis*, Prentice-Hall, Englewood Cliffs, (1966).
- [33] H. Moser, *Proving a manifold to be hyperbolic once it has been approximated to be so*, *Algebra. Geom. Topol.*, **9**, 103–133, (2009).
- [34] K. Murasugi, *On the Alexander polynomial of the alternating knots*, *Osaka Math. J.*, **19**, 181–189, (1958).
- [35] K. Murasugi, *Jones polynomials and classical conjectures in knot theory*, *Topology*, **26**(2), 187–194, (1987).
- [36] R. Patton, *Incompressible punctured tori in the complements of alternating knots*, *Math. Ann.*, **301**, 1–22, (1995).
- [37] G. Perelman, *The entropy formula for the Ricci flow and its geometric applications*, preprint, available at [arXiv:math/0211159](https://arxiv.org/abs/math/0211159).
- [38] G. Perelman, *Ricci flow with surgery on three-manifolds*, preprint, available at [arXiv:math/0303109](https://arxiv.org/abs/math/0303109).
- [39] G. Perelman, *Finite extinction time for the solutions to the Ricci flow on certain three-manifolds*, preprint, available at [arXiv:math/0307245](https://arxiv.org/abs/math/0307245).
- [40] D. Rolfsen, *Knots and Links*, Publish or Perish, Berkeley, Ca, (1976).
- [41] S. M. Rump, *Verification methods: Rigorous results using floating-point arithmetic*, *Acta Numerica*, **19**, 287–449, (2010).
- [42] P. Scott, *The geometries of 3-manifolds*, *Bull. Lond. Math. Soc.*, **15**, 401–487, (1983).
- [43] T. Sunaga, *Geometry of numerals*, Master’s thesis, University of Tokyo, 1956.
- [44] T. Sunaga, *Theory of an interval algebra and its application to numerical analysis*, *RAAG Memoirs* **2**, 29–46, (1958).
- [45] W. P. Thurston, *The geometry and topology of three-manifolds*, notes, Princeton University, Princeton, 1980; available at <http://msri.org/publications/books/gt3m>.
- [46] W. P. Thurston, *Three dimensional manifolds, Kleinian groups and hyperbolic geometry*, *Bull. Amer. Math. Soc.*, **6**, 357–381, (1982).
- [47] Tokyo Institute of Technology, *The Global Scientific Information and Computing Center, Tsubame*, <http://tsubame.gsic.titech.ac.jp/en>.
- [48] Y.-Q. Wu, *Dehn surgery on arborescent knots*, *J. Diff. Geom.*, **43**, 171–197, (1996).
- [49] Y.-Q. Wu, *The classification of toroidal Dehn surgeries on Montesinos knots*, *Comm. Anal. Geom.*, **19**(2), 305–345, (2011).
- [50] Y.-Q. Wu, *Exceptional Dehn surgery on large arborescent knots*, *Pac. J. Math.*, **252**, 219–243, (2011).
- [51] Y.-Q. Wu, *Persistently laminar branched surfaces*, *Comm. Anal. Geom.*, **20**(2), 397–434, (2012).
- [52] Y.-Q. Wu, *Seifert fibered surgery on Montesinos knots*, preprint, available at [arXiv:1207.0154](https://arxiv.org/abs/1207.0154).

DEPARTMENT OF MATHEMATICS, COLLEGE OF HUMANITIES AND SCIENCES, NIHON UNIVERSITY,
3-25-40 SAKURAJOSUI, SETAGAYA-KU, TOKYO 156-8550, JAPAN
Email address: ichihara@math.chs.nihon-u.ac.jp

GRADUATE SCHOOL OF MATHEMATICAL SCIENCES, THE UNIVERSITY OF TOKYO, 3-8-1 KOMABA
MEGURO-KU, TOKYO 153-8914, JAPAN
Email address: masai@ms.u-tokyo.ac.jp